Electromagnetic Non-Destructive Evaluation (XXIII)
G.Y. Tian and B. Gao (Eds.)

doi:10.3233/SAEM200036

Characterization and Imaging of Localized Thickness Loss in GFRP with *Ka*-Band Microwave Open-Ended Waveguides

Jinhua HU[a], Yong LI[a,1], Jianguo TAN[a], Wenjia LI[a] and Zhenmao CHEN[a]
[a]*State Key Laboratory for Strength and Vibration of Mechanical Structures, Shaanxi Engineering Research Centre of NDT and Structural Integrity Evaluation, School of Aerospace Engineering, Xi'an Jiaotong University, Xi'an 710049, China*

Abstract. Glass Fibre Reinforcement Plastic (GFRP) is widely used in engineering fields including aerospace, marine and construction, etc. During practical service, it is prone to the impact damage leading to the Localized Thickness Loss (LTL) which severely influences the integrity and safety of GFRP. To detect and evaluate LTL in GFRP, common Non-Destructive Testing (NDT) techniques such as ultrasonic testing and thermography are usually applied. Complementary to these methods, microwave NDT has been found to be one of the promising techniques in quantitative evaluation of GFRP. In this paper, the characterization and imaging of LTL in GFRP by microwave NDT are intensively investigated. A 2D Finite Element Model (FEM) with the *Ka*-band open-ended waveguide and GFRP sample subject to LTL has been set up and adopted for analysis of field characteristics and testing signals. Following that, an experimental investigation is conducted to further study the feasibility of LTL imaging by microwave NDT with the *Ka*-band open-ended waveguide. The results from simulations and experiments indicate the applicability of *Ka*-band microwave open-ended waveguide for detection and evaluation of LTL in GFRP.

Keywords. Microwave non-destructive testing, localized thickness loss, open-ended waveguide, finite element modelling, average magnitude

1. Introduction

In hash and severe environments, the in-service Glass Fibre Reinforcement Plastic (GFRP) is prone to exterior impact which essentially brings about Localized Thickness Loss (LTL), resulting in structural failure of GFRP [1]. In an effort to secure structural integrity and safety, various Non-destructive Testing (NDT) techniques in GFRP have been developed. However, each of them has drawbacks. Ultrasonic testing requires contact to the testing surface and the detecting range is limited due to the rapid ultrasonic attenuation caused by variation of composite properties [2]. Acoustic emission is costly and needs other NDT methods for re-inspection [3]. X-ray technique is expensive, time consuming and physically damaging [4]. Thermography is limited by insulation property and low thermal conductivity of GFRP composites [5].

Possessed with advantages such as non-contact, low attenuation in non-conductive materials, microwave NDT has been found to be one of the promising complementary to aforementioned NDT methods for evaluation of such dielectric materials as GFRP. Hosoi

[1] Corresponding Author, Yong Li, State Key Laboratory for Strength and Vibration of Mechanical Structures, Shaanxi Engineering Research Centre of NDT and Structural Integrity Evaluation, School of Aerospace Engineering, Xi'an Jiaotong University, Xi'an 710049, China; E-mail: yong.li@mail.xjtu.edu.cn.

et al. utilized focusing mirror sensor, detected the 100-μm-thick delamination in 3-mm-thick GFRP laminate [6]. Moreover, by measuring the variation in the amplitude of the microwave reflectivity, a 7.5-μm-thick film was detected in a 3-mm-thick GFRP laminate [7]. Ryu et al. successfully detected and revealed hidden multi-delamination in GFRP laminates using reflection method with THz-TDS imaging system [8]. Sutthaweekul et al. adopted principle component analysis and synthetic aperture radar tomography to evaluate the depth of flat-bottom holes in coated GFRP pipes [9].

Following the research of microwave NDT for GFRP evaluation, in this paper the feasibility of *Ka*-band microwave open-ended waveguide for characterization and detection of LTL in GFRP is investigated through simulations and experiments. A 2D Finite Element Model (FEM) is established to investigate the relations between the reflection parameters i.e., S_{11} and the LTL size. Meanwhile, experimental investigation with the *Ka*-band microwave open-ended waveguides is performed to explore the imaging of LTL in GFRP plates. An image processing algorithm based on the high-pass filtering and normalization is proposed to mitigate the influence of background noise and enhance the detectability of LTL in GFRP.

2. Numerical Simulations via FEM

For the transverse electric (TE_{mn}) wave in a microwave waveguide, the component of electric field in the direction of propagation vanishes. Further, for the transmission of the TE_{10}-mode microwave in rectangular waveguide, the electric-field component in the direction along the long side (m=1) of rectangular waveguide is zero, and the one along the short side (n=0) is independent of the coordinate in the corresponding direction [10]. Hence, the 3D model of microwave NDT is thus simplified into 2D.

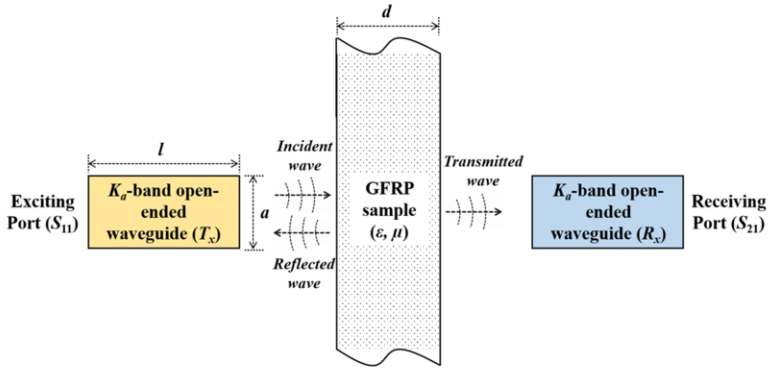

Figure 1. 2D model for inspection of a GFRP sample with *Ka*-band open-ended waveguides

The schematic of the 2D model is presented in Figure 1. Considering the aperture size (7.11mm×3.56mm) and length (l=214mm) of the waveguide, in the 2D FEM a=7.11mm. The thickness of the GFRP plate is 6mm. The parameters for LTL defects are set with the diameters (D) from 5mm to 13mm and depths (d) from 2mm to 6mm. The lift-off distance between the waveguide aperture and surface of the GFRP plate is 3mm. The excitation frequency of the waveguide is set as *Ka*-band (30GHz-40GHz). During simulations, the waveguide scans over the GFRP sample with the spatial interval of 0.3mm. At each scanning position, S_{11} against the excitation frequency is acquired. The Average Magnitude (AM) [9] of S_{11} in different scanning positions (X position) is obtained, which eventually gives the scanning curve of LTL. The simulated scanning

curves are shown in Figure 2. It can be observed from Figure 2 that: (1) S_{11} AM varies with the scanning positions, indicating the presence of LTL; and (2) the scanning curve changes with the LTL size. This implies that S_{11} AM could be applicable for LTL detection and quantitative evaluation of LTL size.

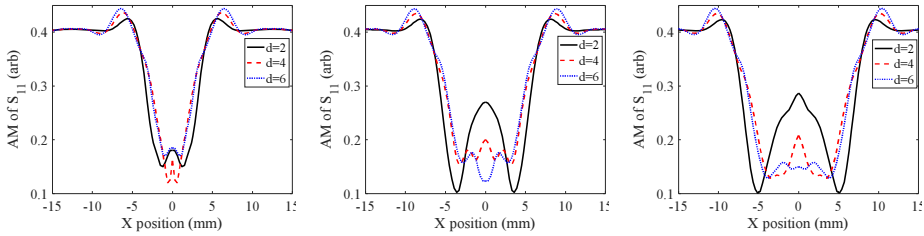

(a) D=5mm (b) D=10mm (c) D=13mm

Figure 2. Simulated scanning curves for different LTLs

From the scanning curves, the S_{11} AM at X=0 (corresponding to the LTL centre) is extracted and used for the measurement of LTL depth. The relationship between S_{11} AM and LTL depth is shown in Figure 3. It can be seen from Figure 3 that the S_{11} AM tends to monotonically decrease with the LTL depth. The reasoning could be due to the fact that larger LTL depth diminishes the equivalent relative permittivity [11] of the GFRP sample, which directly results in the decrease of microwave reflection from interfaces and thus the smaller magnitude of S_{11}. As for the evaluation of LTL diameter, the spatial span of minimum values of S_{11} AM in each curve is chosen as the signal feature to estimate the diameter for each LTL. The correlation relation between the spatial span and LTL diameter is presented in Figure 4. It can be seen from Figure 4 that the spatial span is directly proportional to the LTL diameter. Since the minimum S_{11} AM manifests at the edge of LTL due to the large microwave scattering at the LTL edge, as the diameter of LTL increases, the spatial span of minimum values of the scanning curve consequently rises, giving the increasing tendency.

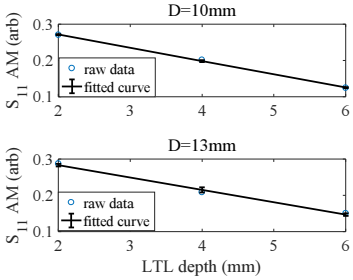

Figure 3. S_{11} AM *vs.* LTL depths

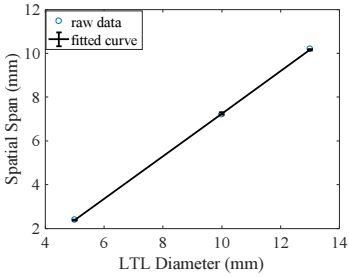

Figure 4. Spatial span *vs.* LTL diameters

3. Experimental investigation

In order to further investigate the feasibility of quantitatively evaluating LTL size by *Ka*-band microwave NDT, a microwave testing system has been set up. The system schematic is shown in Figure 5. The system consists of a Vector Network Analyser (VNA) for excitation of the incident wave and measurement of S_{11}, *Ka*-band open-ended waveguide for transmitting and receiving the TE_{10} mode electromagnetic wave, and scanning stage for the automatic 2D scanning of a GFRP sample with LTL in different sizes (D=5~13mm, d=2~6mm). The experimental parameters are listed in Table 1.

Table1. Experimental parameters

Waveguide aperture size	7.11mm×3.56mm
Scanning area	220mm×40mm (2D scanning)
Frequency range	30-40GHz (*Ka*-band)
Number of sampling frequency	201 (Δf=50MHz)
Lift-off	5mm
Scanning step sizes	Δx=Δy=1mm

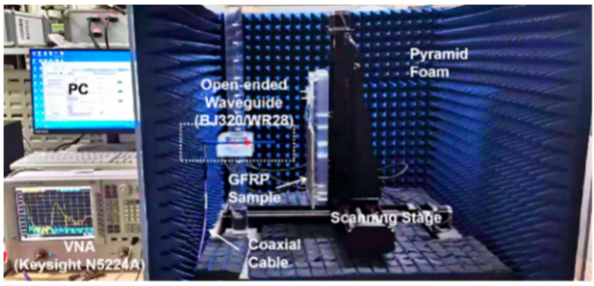

Figure 5. Experimental set-up

3.1. LTL imaging results and processing

The 2D scanning of the waveguide over the sample is carried out along with acquisition of the S_{11} AM at every scanning position. Figure 6 shows the imaging results. The detected LTLs are 5mm, 10mm and 13mm in diameter in the three subgraphs from top to bottom, while the depths of LTLs in each subgraph are 2mm, 4mm and 6mm from left to right. It can be found from Figure 6 that all the LTL defects are successfully detected. However, the imaging results are severely influenced by the strong background noise which could be due to extraneous wave reflections in the testing region. This gives rise to much difficulty in LTL evaluation.

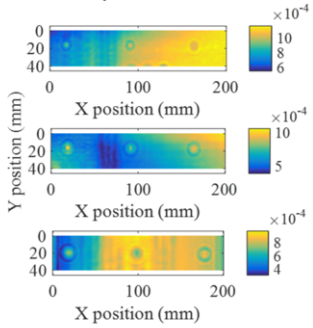

Figure 6. Raw imaging results

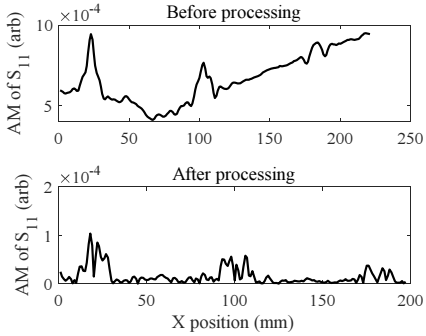

Figure 7. Scanning curves along the centre of LTLs

Considering the fact that the background noise is mostly low-frequency, a processing algorithm based on the high-pass filtering together with normalization is proposed and utilized to mitigate the influence from the background noise. Normalization was conducted by obtaining the ratio between the S_{11} AM in each scanning position and the largest S_{11} AM of all the scanning areas. Figure 7 presents the comparison of the scanning curves along the centre of LTLs with and without processing. It is noticeable from Figure 7 that without processing, the background noise is rather strong. In contrast, after processing, S_{11} AM in flawless area is suppressed to a certain

extent, resulting in higher indication regarding the LTL presence. Figure 8 illustrates the processed LTL images. From Figure 8, it can be observed that the processed S_{11} AM changes with the LTL depth, the larger of the depth, the smaller of the S_{11} AM. The comparison between Figure 6 and Figure 8 indicates that the imaging processing method benefits the detection and sizing of LTL.

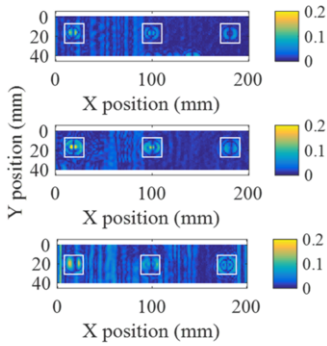

Figure 8. Processed imaging results

3.2. LTL characterization

After being detected via *Ka*-band microwave imaging, the LTLs are subsequently characterized by analysing the correlations between the image feature and LTL size. The sum of normalized S_{11} AMs i.e., ΣS^{N}_{11}(AM) in a 20mm×20mm observation window (indicated by the square in Figure 8) whose centre coincides with the LTL centre is computed and taken as the image feature for analysis. Thereafter, for LTLs with the same diameter/depth, linear fitting method was adopted to explore the correlations of ΣS^{N}_{11}(AM) with the depth/diameter of LTL. Figures 9 and 10 exhibit the results. It is noted that in calculating the maximum relative errors between experimental ΣS^{N}_{11}(AM) and fitted ones are 14.07% (D=13mm) as LTL depth changes, and 16.83% (d=2) as LTL diameter changes, respectively.

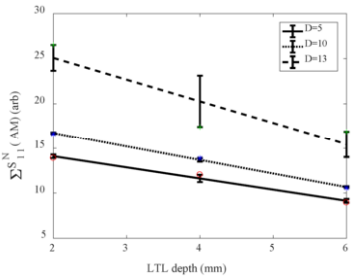

Figure 9 ΣS^{N}_{11}(AM) *vs.* LTL depths

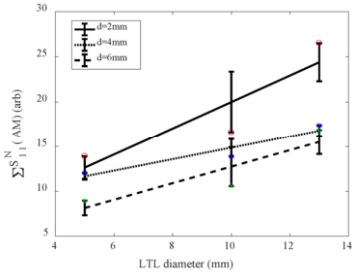

Figure 10 ΣS^{N}_{11}(AM)*vs.* LTL diameters

From Figures 9 and 10, it can be seen that ΣS^{N}_{11}(AM) has a monotonic relation with the LTL depth/diameter. It decreases as the LTL depth enlarges. In contrast, when LTL diameter rises, ΣS^{N}_{11}(AM) increases. This is supportive of the derived correlation from numerical simulations. As mentioned in Section 2, the larger of the depth, the smaller of the equivalent relative permittivity of the GFRP sample and the smaller of the S_{11}

magnitude. Meanwhile, the larger of the LTL diameter, the larger of ΣS^{N}_{11}(AM) because of the broader interface (air and GFRP).

4. Conclusions

In the paper, the detection and characterization of LTL in GFRP plates via *Ka*-band microwave open-ended waveguide is intensively investigated through simulations experiments. It can be concluded from the results that: (1) with the *Ka*-band microwave open-ended waveguide, LTL in GFRP can be localized and evaluated; (2) the processing algorithm proposed based on the high-pass filtering and normalization is applicable for the background removal and LTL sizing; and (3) ΣS^{N}_{11}(AM) has monotonic correlations with the LTL depth and diameter, which benefits the quantitative evaluation of LTL in GFRP. Following the current work, further study will involve: (1) investigation with small-sized/pitting LTL; and (2) detection and characterization of LTL in the back side of GFRP plates.

Acknowledgments

The authors would like to thank the National Natural Science Foundation of China (Grant Nos. 51777149, 11927801), National Key R&D Program of China (Grant No. 2017YFF0209703), and Fundamental Research Funds for the Central Universities of China (Grant No. XJJ2018027) for funding this research.

References

[1] Na WS. Possibility of detecting wall thickness loss using a PZT based structural health monitoring method for metal based pipeline facilities. *NDT & E International*. 2017 Jun;88:42-50.
[2] Castellano A, Fraddosio A, Piccioni MD. Quantitative analysis of QSI and LVI damage in GFRP unidirectional composite laminates by a new ultrasonic approach. *Composites Part B: Engineering*. 2018 Oct;151:106-117.
[3] Kumar PK, Kuppan P. Online monitoring of delamination mechanisms in drilling of Mwcnts reinforced Gfrp nanocomposites by acoustic emission. *Materials Today*: Proceedings. 2018;5(5):13036-13047.
[4] Humer K, Spieβberger S, Weber HW, Tschegg EK, Gerstenberg H. Low-temperature interlaminar shear strength of reactor irradiated glass-fibre-reinforced laminates. *Cryogenics*. 1996 Aug;36(8):611-617.
[5] Palumbo D, Cavallo P, Galietti U. An investigation of the stepped thermography technique for defects evaluation in GFRP materials. *NDT & E International*. 2019 Mar;102:254-263.
[6] Hosoi A, Yamaguchi Y, Ju Y, Sato Y. Detection of delamination in GFRP and CFRP by microwaves with focusing mirror sensor. *Material Science Forum*. 2013 Mar;750:142-146.
[7] Hosoi A, Yamaguchi Y, Ju Y, Sato Y, Kitayama T. Detection and quantitative evaluation of defects in glass fiber reinforced plastic laminates by microwaves. *Composite Structures*. 2015 Sep;128:134-144.
[8] Ryu CH, Park SH, Kim DH, Jhang KY, Kim HS. Nondestructive evaluation of hidden multi-delamination in a glass-fiber-reinforced plastic composite using terahertz spectroscopy. *Composite Structures*. 2016 Nov;156:338-347.
[9] Sutthaweekul R, Tian GY, Wang Z, Ciampa F. Microwave open-ended waveguide for detection and characterization of FBHs in coated GFRP pipes. *Composite Structures*. 2019 Oct;225, Article No. 111080.
[10] Ida N. Microwave NDT. London: Springer; 1992. p.75-77.
[11] Ghodgaonkar DK, Varadan VV, Varadan VK. Free-Space measurement of complex permittivity and complex permeability of magnetic materials at microwave frequencies. *Transactions on Instrumentation and Measurement*. 1990 Apr;39(2):387-394.